The Effects of Chemical Pressurization on Screen Electrode Fuel Cells

by

Ali Ahmed

SUBMITTED TO THE DEPARTMENT OF MECHANICAL ENGINEERING IN
PARTIAL FULFILLMENT OF THE REQUIREMENTSFOR THE DEGREE OF

BACHELOR OF SCIENCE
AT THE
MASSACHUSETTS INSTITUTE OF TECHNOLOGY

JUNE 2007

Signature of Author..
Department of Mechanical Engineering
May 9, 2007

Certified by..
Ernest G. Cravalho
Professor of Mechanical Engineering
Thesis Supervisor

Accepted by..
John H. Lienhard V
Professor of Mechanical Engineering
Chairman, Undergraduate Thesis Committee

1

The Effects of Chemical Pressurization on Screen Electrode Fuel Cells

by

Ali Ahmed

ABSTRACT

A large amount of fuel cell research focuses on porous gas diffusion (PGD) fuel cells which currently produce the best power density. However, this sect of fuel cell technology has many obstacles to overcome before becoming a viable large scale source or power. Nevertheless, alternatives to PGD fuel cells exist. Fluidized bed electrodes (FBE), packed bed electrodes, and packed screen electrodes are discussed and analyzed in this thesis. Fluidization provides a number of benefits, but also presents a different set of obstacles. One of the largest benefits of fluidization is the possibility of using chemical pressurization to increase the reactant concentration. Perfluorocarbons (PFC), currently being used in biomedical applications as oxygen carriers in plasma, can be used to effectively raise the cathode oxygen concentration.

This thesis will propose a model of perfluorocarbon emulsions as applied to an oxygen half cell. The model is first developed for the simple case of a rotating disk electrode (RDE). The predictions of this model are then compared with data obtained from a RDE experiment with and without the use of PFC's. The model is then extended to the use of packed screen electrodes. The key findings of the model include the relationships between bed length, power output, oxygen concentration, and volumetric flow rate. Finally, the thesis is concluded with a description of the setup created to test the predictions of the model and proposals for future extensions of this research.

Thesis Supervisor: Ernest G. Cravalho
Title: Professor of Mechanical Engineering

Table of Contents

1.0 Introduction

Current energy consumption in the world is at an all time high with the increased use of fossil fuels for transportation in industrialized countries and the expanded use of energy consuming processes within developing countries such as China and India. The market has reacted with increased production and higher prices [1]. The United States, in an attempt to soften the domestic use of fossil fuels has enacted strict standards of consumption in industry. Increasingly stringent Corporate Average Fuel Economy (CAFE) standards affect mile per gallon requirements of automotive manufacturers in an attempt to increase efficiency in the transportation industry [2]. All of these factors combine to create strong initiatives toward researching methods of efficiency increasing technology and alternative technologies that meet these economic and legal demands. Some of these efforts include hybrid, regenerative, ethanol, and hydrogen technology.

Despite the rising costs of fossil fuels, they are still relatively cheap when compared with alternative energy production methods. Nevertheless, as costs rise, doors are opened for technologies that were previously too expensive to be feasible. The clearest examples are the use of ethanol and bio-diesel for use in current automobiles. A lot of focus is placed on generating efficiency gains in internal combustion engines, but as fossil fuel costs rise, more research will be performed on alternative means of power generation. Electric vehicles now exist that exhibit performance characteristics of ICE vehicles but with much greater efficiency, maintaining an effective 135 mpg according to the Tesla Motors website. Another example of this paradigm shift is apparent in the research efforts of fuel cell technology. Electric transportation and fuel cell technology both exhibit cost disadvantages, but they are fledgling technologies and have opportunities to increase efficiencies and lower costs due to materials engineering and economies of scale [3]. In addition, these technologies provide a much cleaner burning means of energy production which is also an important consideration legally and environmentally.

Many types of fuel cell technologies exist, and opportunities for advancement exist not only in the research of new types of fuel cells, but also in the progression of the more mature types of fuel cells. Nevertheless, current fuel cell technology produces inferior power output compared to more conventional means of energy production. Advances need to be made in fuel cell technology to make it a viable alternative and eventually a replacement for current technologies [4].

Many types of fuel cells currently exist for a variety of different applications ranging from large scale industrial energy production to use in portable electronic devices. Most research of fuel cell technology for vehicles and portable devices has been conducted on porous gas diffusion (PGD) or proton exchange membrane fuel cells (PEMFC) [5]. This is a proven technology that is currently in the stages of optimization and cost reduction [6, 7, 8, 9]. Other efforts have been in the realm of development of newer technology. "Direct methanol fuel cell (DMFC) development (usually for portable or mobile products) has accelerated, with the number of companies and other organization involved increasing rapidly" [5]. Research has been focused on mitigating the limitations of the design such as carbon dioxide poisoning and costs [10, 11]. Other research has gone into

advancing even older technology including alkaline fuel cells (AFC) [13, 14] that has "fallen out of favour with the technical community in the light of the rapid development of the Proton Exchange Membrane Fuel Cells" [12], addressing long term life cycles and computational optimization.

2.0 Fuel Cell Electrode Chemistry

The general reaction governing fuel cell chemistry is the formation of water from hydrogen and oxygen

$$H_2 + \frac{1}{2}O_2 = H_2O \tag{1}$$

The two half cell reactions are

$$H_2 + 2OH^- = 2H_2O + 2e^- \qquad E = .83V \tag{2}$$

$$\frac{1}{2}O_2 + H_2O + 2e^- = 2OH^- \qquad E = 1.23V \tag{3}$$

In an electrochemical cell, there are three primary irreversibilities or overpotentials. The first is the activation overpotential. The second is the ohmic overpotential resulting from the resistance to ion transport within the electrolyte between the anode and cathode of the cell. The third, concentration overpotential, is due to the mass transport limitations of getting the electrochemical reactants to the catalyst surface [15]. The three overpotential regions are illustrated in Figure 1.
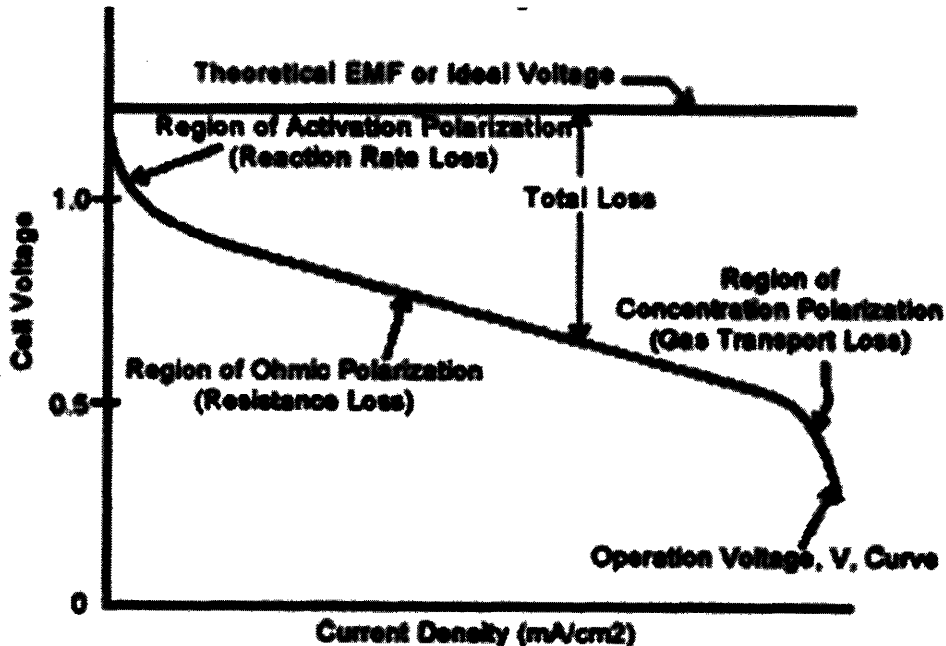
Figure 1. Illustration of three overpotential regions of electrochemical cell.

Each of the overpotential regions is a function of a different design parameter of the cell. The activation potential is determined by the catalyst used and the reactants and has relatively little electrode design influence. The other two overpotential regions are a function of the design parameters of the cell. For the purposes of this research we will focus on the mass transport limitations of the fuel cell.

5

The goals of this thesis include:

1.   Presenting an overview of limitations of current fuel cell technologies.
2.   Proposing the use of Perfluorocarbons (PFC's) to increase cell performance by chemical pressurization.
3.   Developing a model of the benefits to using PFC's in rotating disk electrode (RDE) applications.
4.   Presenting results of RDE experiment and compare to model.
5.   Developing a model for packed screen electrodes using PFC's to chemically pressurize the cell.
6.   Presenting novel screen electrode setup and propose future research and extensions of developed model

2.1 Brief Description of PGD Technology and Limitations

PGD fuel cells follow the equations presented above, using oxygen and hydrogen gas passed over a porous membrane at the cathode and anode, respectively. The gases diffuse into the membrane, and react with the catalyst that coats the pores. The membrane is used as the ion transport mechanism between the two half cells and electrons are collected from the anode, used to perform work, and returned to the cathode as depicted in Figure 2 reproduced from [15]
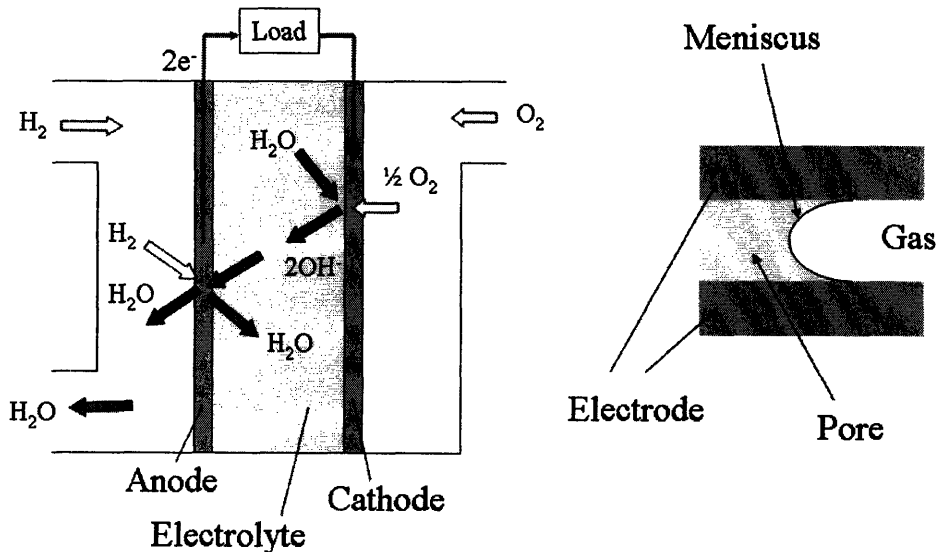
Figure 2. "Left-hand side of figure is a schematic of the general configuration and reactions of an alkaline electrolyte fuel cell. The right-hand side shows a simplified depiction of the porous electrode structure, highlighting the meniscus formed at the interface of the electrolyte and reacting gas." [15]

Even though this type of fuel cell technology is very prevalent in industrial research and applications, it is susceptible to a variety of performance limitations. First, the design parameters of the electrode pores cause the costs of the electrodes to be extremely high due to complicated fabrication techniques [3, 16]. In addition, the platinum catalyst

within the electrode pores can be poisoned by carbon dioxide causing the membrane to become less efficient and eventually nonfunctional. Also, despite the high cost of precision fabrication, the full catalyst surface is not utilized. Current state of the art fabrication technology still only allows for about 40% of the platinum surface to be utilized as a catalyst [17]. In addition, PGD electrodes are also subject to clogging, water management issues, and other long term cost factors [15].

2.2 A Fluidized Approach

In order to mitigate some of the issues of PGD electrodes, a fluidized approach may be used. Current fluidized electrodes cannot produce nearly the same efficiency or power density as PGD or PEM electrodes, however, because of their lower likelihook of being poisoned, lower cost of reversing poisoning, lower cost of fabrication, ability to last longer, and their potential to be more robust, there is hope for the progression of the technology.

2.2a Fluidized Bed Electrodes (FBE)

Both two and three phase FBE's have been researched to provide sufficient reactant to the catalyst site and utilize a larger portion of the catalyst area [16, 18]. A simple setup of an FBE is shown in Figure 3 [15]
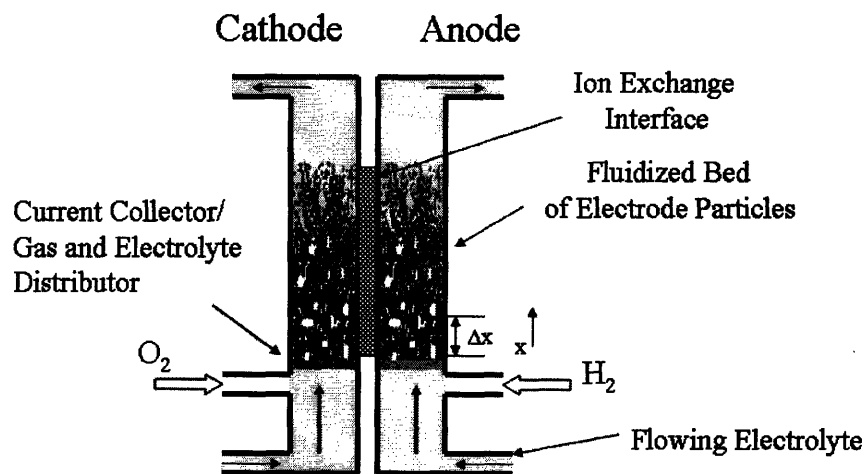
Figure 3. Simple model of Fluidized Bed Electrode (FBE) [15]

Current research has shown that the limitations of the FBE model include trying to achieve high surface area where the reaction is occurring [16, 18]. Additionally, the desire of a fluidized bed is to have the particles suspended by the flow of the fluid providing good mass transport and high surface area, but the problem arises of maintaining contact between the particles and the electrode. If the particles become charged, they become temporarily inactivated. Also, the concentration of oxygen decreases as the electrolyte flows through the bed. The use of a three phase fluidized bed attempts to keep the concentration of oxygen at the saturation concentration while also agitating the bed to increase mass transport. Raney particles were also used to increase the surface area of the catalyst [16, 18], but proved to be ineffective when the results were analyzed by Ruflin [15].

7

2.2b Packed Bed Electrodes

Packed bed electrodes consist of a fluidized bed electrode restricted to a fixed length by hindering the movement of the particles. This maintains the contact of the particle with the electrode to overcome the problem of the particles disconnecting from the bed as they do in FBE's. However this method of constant contact reduces surface area relative to the FBE case and there is still the problem of maintaining a high oxygen concentration throughout the length of the electrode.

2.2c Screen Electrodes

Similar to packed bed electrodes, screen electrodes allow for complete contact of the reaction site with the electrode. Nevertheless, it is much easier to optimize the parameters governing the half cell because of the uniform nature of the screen in terms of packing and there is also the ability to control the orientation of the reaction surface relative to the electrolyte flow and the other screens in the packed bed. Holeschovsky et al. notes the merit of using screen electrodes for comparison with theoretical models because of their accurately known internal surface area and simple geometry [19]. For the reasons of control and modeling, screen electrode half cells will be the focus of this thesis.

2.3 Application of Chemical Pressurization to Fuel Cells

It is apparent from the discussions about the limitations of each type of fuel cell design that a constant limitation is the ability to get reactant to the catalyst site. Clearly it is beneficial to drive more reactant to the catalyst because this produces a higher current output which in turn produces a higher power output and power output density for the cell. For the purposes of this thesis, the focus will be on the oxygen half cell (cathode).

The method used in this thesis to bring more reactant to the site of reaction is to use a perfluorocarbon(PFC) emulsion to chemically pressurize the electrolyte. PFC's are able to dissolve about twenty times more oxygen than water or a solution of KOH. Previously, perfluorocarbons have been used in biomedical research to chemically pressurize blood and have successfully been used in animals as a fluidized oxygen transport mechanism [20, 21]. Research has shown that the mass transfer resistance across the interface of the emulsion is insignificant [3]. This research suggests that when applied to a similar fluidized oxygen transport system, perfluorocarbons will be very effective and lead to significant power output density improvements over fluidized bed electrodes. The optimization problem is essentially getting as much power out of the cell as possible after netting it against the power required to pump the electrolyte through the cell. By dissolving orders of magnitude more oxygen in the same electrolyte stream, the output of the cell can be increased without increasing the pump's power consumption. The use of perfluorocarbons overcomes the limitations of mass transport around the electrode catalyst by supplying more oxygen to the reaction sites and increases the

8

overall efficiency of the cell. This decreases the effects of the concentration overpotential, allowing for a much larger limiting current and power output.

3.0 Rotating Disk Electrode

Rotating disk electrodes(RDE) can provide an easy way to analyze the benefits of using a perfluorocarbon emulsion to chemically pressurize oxygen in the potassium hydroxide electrolyte. A simplistic model will be presented to show the benefits of using PFC's and some of the limitations of the model will be discussed.

As noted by Prentice et al, rotating disk electrodes offer a number advantages over standard electrode setups. The diffusion layer of the electrolyte over the electrode is uniform and controllable using an RDE. In addition, the system is well defined mathematically [22]. The definition of the diffusion layer thickness (δ) as giving in [22] attributes to Levich the following equation:

$$\delta = 1.61(D^{0.333})(\gamma^{0.167})(\omega^{-0.5}) \tag{4}$$

where (D) represents the diffusion coefficient of the reactant, (γ) stands for the kinematic viscosity of the solution, and (ω) is the angular velocity of the disk [22].

The current that is produced by an electrode is given by

$$i = nFAD\frac{dC}{dx} \tag{5}$$

where (n) is the number of electrons produced from the reduction reaction, (F) is Faraday's constant, (A) is the surface area of the electrode, (D) is the diffusion coefficient of the reactant, (C) is the concentration of reactant, and (K) is a conversion constant. When using the RDE to analyze a dissolved oxygen solution, there are two reduction pathways that are possible for the oxygen molecule. The first is a full reduction (n = 4) of oxygen to hydroxide ions. The other reduction reaction (n = 2) does not fully reduce oxygen and thus creates hydrogen peroxide.

$$O_2 + 2H_2O + 4e^- = 4OH^- \qquad E = .495V \tag{6}$$

$$O_2 + 2H_2O + 2e^- = 2H_2O_2 \qquad E = -.041V \tag{7}$$

In addition, there is an additional reaction within the electrode in which water is being reduced to form hydrogen gas and hydroxide ions. This reaction, however, following from (5) does not have a concentration gradient because the concentration of water everywhere in the RDE is constant. If we assume that the concentration profile within the small laminar diffusion layer is linear, we can replace the differential term with $\Delta C/\Delta x$ which can be approximated to

9

$$\frac{(C_{bulk} - C_{surface})}{\delta} = \frac{C_{bulk}}{\delta} \tag{8}$$

Combining (4), (5), and (8), we arrive at an expression for the current in a rotating disk electrode

$$i = .621(n)(F)(A)(D^{0.667})(\gamma^{-0.167})(\omega^{0.5})(C_{bulk}) \tag{9}$$

What is important to take from this model is that the current output of the RDE is proportional to the square root of the angular velocity and directly proportional to the concentration of the oxygen in the electrolyte. As noted above, the contribution to the total current that is due to the reduction of water can be negated by looking at the change in current due to a change in oxygen concentration, however, for the purposes of this thesis, the rate of the water reduction reaction is assumed to be insignificant relative to the reduction of both the oxygen saturated electrolyte and the saturated perfluorohexane emulsion.

3.1 Extension of RDE Model to PFC emulsion

In order to extend the RDE model to the perfluorohexane emulsion, we must analyze which components of equation (9) are altered. Clearly, since PFC's are able to dissolve approximately 20 times more oxygen than water alone, the bulk concentration term will be affected. In addition, the surface area of the electrode (A) may also be changed. Only a portion of the surface area of the electrode will be covered by PFC. The remaining portion of the surface area will be covered by electrolyte. Each case will be analyzed individually.

The first case involves letting the area term remain equal to the entire surface area of the RDE and altering the effective concentration of oxygen to account of the characteristics of the emulsion. If we define (C_{eff}) as the effective concentration, then

$$C_{eff} = \chi(C_{PFC}) + (1 - \chi)(C_{bulk}) \tag{10}$$

where (C_{PFC}) is the concentration of oxygen dissolved in the perfluorocarbon, (C_{bulk}) still represents the bulk concentration of oxygen in the electrolyte, and (χ) represents the volume fraction of the solution that is PFC. For the purposes of this model, the volume fraction of the surfactant is neglected. PFC's tend to dissolve 15-20 times more oxygen than water or electrolyte [23,24]. Therefore, we can rewrite (10)

$$C_{eff} = (C_{bulk})[1 - \chi(1 - f)] \tag{11}$$

where (f) represents the ratio of concentration in the PFC to the bulk concentration of oxygen in the electrolyte. Combining equations (9) and (11) yields an overall equation

10

for the limiting current in the RDE under the assumption that equation (11) accurately reflects the overall effective concentration of the solution.

$$i = .621(n)(F)(A)(D^{0.667})(\gamma^{-0.167})(\omega^{0.5})(C_{bulk})[1 - \chi(1 - f)] \tag{12}$$

Equation (12) can be used to infer (f) if (i) is known, allowing us to determine the amount of oxygen dissolved in the PFC alone.

Additionally, the system could be modeled so that the concentrations of oxygen in the PFC and the bulk electrolyte are known but the contact profile of the PFC on the electrode is unknown.

The number of drops in the entire mixture can be determined by

$$N = \frac{(\chi)(V)}{\pi(R^2)} \tag{13}$$

where (R) is the radius of each PFC droplet. This radius can be controlled by sonicating the emulsion and then analyzing it with a microscope. After sonicating, the sample exhibits minimal Oswald Ripening even after 42 days [21]. The probability that any one drop is in contact with the electrode surface is given by

$$\Pr(contact) = \frac{2R}{w + 2R} \tag{14}$$

In the limiting case of the droplet size being much larger than the width, the probability of contact becomes 1. On the other hand, when the width is much larger than the droplet size, the probability of contact becomes (2R/w). When (w) and (R) are on the same order of magnitude,

$$\Pr(contact) = \frac{2R}{w + 2R} \cong \frac{R}{w} = \frac{RA}{V} \tag{15}$$

The average contact surface of each droplet is given by

$$a = \frac{1}{R}\int Adr = \frac{1}{R}\int 2\pi r dr = (\frac{1}{R})(\pi r^2)\Big|_{0}^{R} = \pi R \tag{16}$$

From this point, if we multiply the number of drops in the entire solution by the probability that any one of those drops is in contact with the surface of the electrode by the average cross-sectional area of each drop with the contact surface, we will arrive at the total area of the electrode covered by the PFC droplets. The remaining area of the electrode will be wetted by the electrolyte. Combining each of these concepts,

$$A_{PFC} = N * \Pr(contact) * a \cong \frac{(\chi)(V)}{\pi(R^2)} * \frac{RA}{V} * (\pi R) = \chi A \qquad (17)$$

The effective area subject to the "bulk" concentration is given by

$$A_{eff} = A_{Bulk} + f(A_{PFC}) = (A - A_{PFC}) + f(A_{PFC}) = (A - \chi A) + f(\chi A) = A[1 - \chi(1 - f)] \qquad (18)$$

Plugging this into (9) yields the exact same equation as (12). The key differences were in the assumptions made about the effective concentration in the first model and the assumptions about the contact probability and area in the second model. In a more complex model, the concentration gradient within the PFC droplet and the possible deformation due to the droplet being forced against the plate would be incorporated. Nevertheless, the similar result in both of these models will help in the analysis of the rotating disk electrode data.

4.0 Rotating Disk Electrode Experiment

The equipment, preparation, and parameters of the RDE experiment will be outlined in this section. This will be followed by a prediction of the findings from the model presented in the previous section. Subsequently, the data from the RDE experiment will be presented and analyzed for any possible sources of discrepancy between the model of how the PFC emulsions should behave and how they actually performed.

4.1 RDE Experimental Setup

The RDE used in the experiment was an adjustable speed rotator with a platinum electrode purchased from Pine Research Instrumentation.
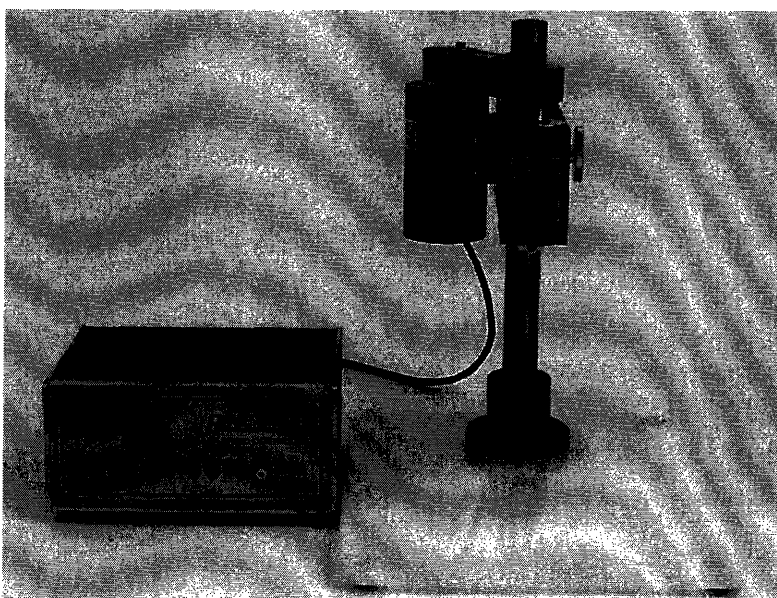
Figure 4. Pine Research Instrumentation ASR Rotator used with platinum RDE

The perfluorocarbon used was a n-perfluorohexane 99% pure from Sigma Aldrich. The surfactant used was a fluoro-link surfactant obtained from Survey Solexis. The electrolyte was a 0.5 M potassium hydroxide (KOH) from Sigma Aldrich.

A single perfluorohexane solution was created for all the tests performed in the RDE. To create the solution, 25 mL of perfluorohexane were added to 100mL of 0.5 M KOH. Then, 2 mL of fluoro-link surfactant was added to the solution. The solution was shaken by hand for 2 minutes then allowed to settle for 5 minutes. An additional mL of surfactant was added to the emulsion for a total of 3mL of surfactant. After shaking again, the emulsion had not separated after 15 minutes. The solution was then sonicated for 20 minutes. The droplet size was not measured by microscope since the same emulsion was used in all of the trials and the droplet size from equation (17) plays a small role, if any, in the limiting current.

The datasets that were recorded when using the RDE were current vs. potential plots for which the region of most interest is the limiting current. This region is most attributable to the mass transport overpotential. The RDE was run at three different speeds, 360 rpm, 2360 rpm, and 4360 rpm. At each speed, two samples were run in the RDE, one with 0.5 M KOH and the other with the perfluorohexane emulsion described above.

4.2 Predictions of RDE Model

The model created in 3.1 can be used to predict the relative limiting currents between each of the samples. First, for each solution, the relative values of the limiting current can be predicted by equations (9) and (12). For the standard electrolyte solution, equation (9) would predict that the limiting currents of the 2360 rpm and the 4360 rpm solution relative to the 360 rpm solution would be

$$i_{4360} = \sqrt{\frac{4360}{360}}(i_{360}) = 3.48(i_{360}) \quad (19) \qquad i_{2360} = \sqrt{\frac{2360}{360}}(i_{360}) = 2.56(i_{360}) \quad (20)$$

Also, since solution of the same composition is being used in all three speeds for the PFC runs on the RDE, the volume fraction (χ) and the relative oxygen concentration (f) terms are constant for all three samples. So, the same relationship that applies to equation (12) also applies to equation (9). The relative currents in the PFC emulsion runs should follow the relationships in (19) and (20).

In addition, we can make a prediction about the benefit of using the PFC emulsion over the electrolyte alone. Figure 5 shows the effects of the volume fraction (χ) and the relative oxygen concentration (f) on current output.
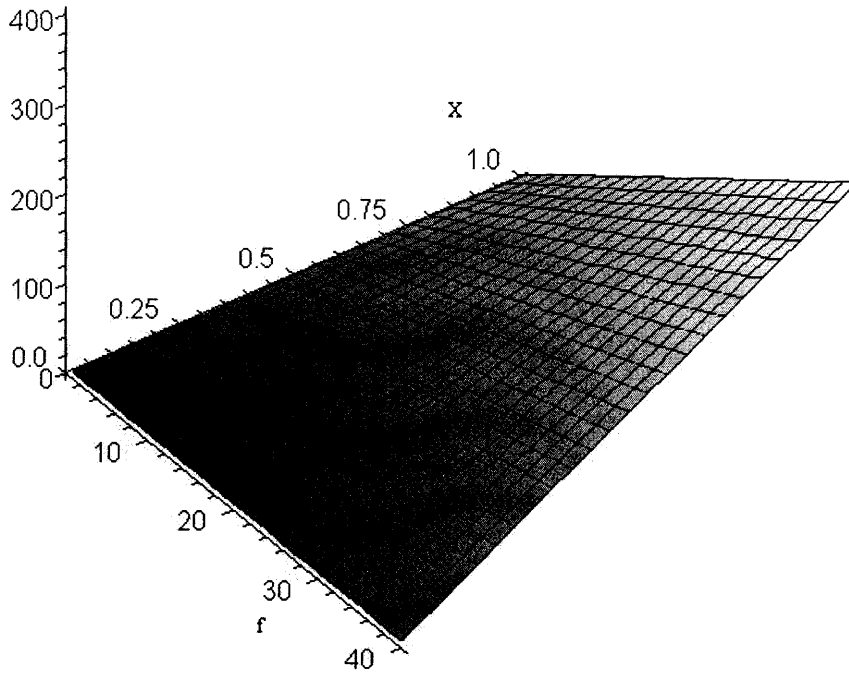
Figure 5. Graphical representation of equation (12) showing current on the z axis as a function of PFC volume fraction (χ) and the relative oxygen concentration (f)

Given the model, using a 100% PFC solution would produce the highest current, but in reality, there is an ion transport mechanism that requires electrolyte to carry the products of the reduction reaction away from the electrode site. Because of this need for electrolyte, a pure PFC solution cannot be used. The solution that was made for this experiment consisted of 25 mL of perfluorohexane dissolved in 100 mL of .5M hydroxide solution using 3mL surfactant.

$$\chi = \frac{25}{100 + 25 + 3} = \frac{25}{128} = .1953 \approx .195 \tag{21}$$

Furthermore, for perfluorohexane, the relative oxygen concentration is approximately 15-20 times more than the oxygen concentration of pure water or electrolyte [23, 24]

$$\frac{i_{PFC}}{i_{OH}} = [1 - \chi(1 - f)] \tag{22}$$

Given these values for χ and f, a prediction for the benefit from using perfluorohexane can be made. Equation (22) divides equation (12) by (9). From this, it can be seen that the ratio of the current in the PFC case to the electrolyte-only case is a function of χ and f. For the values given above, the PFC emulsion should provide between 3.75 and 4.75 times as much limiting current as the solution of electrolyte alone.

4.3 Results of the RDE experiment

As described above, six solutions were run using the RDE electrode, the details of which are in Table 1.

Table 1. Solutions used in RDE experiment. Each solution is .5M KOH. For those with perfluorohexane added, the volumetric fraction is .195.

Solution	RPM	PFC	i_{lim} (mA)
1	4360	Yes	2.03
2	4360	No	1.11
3	360	Yes	0.722
4	360	No	0.423
5	2360	Yes	1.611
6	2360	No	0.9815

The results of the experiment are in the form of a current versus voltage plot. The three overpotential regions can be seen in the plots, but for the purposes of this experiment, the limiting current as the magnitude of voltage increases is of importance. Figure 6 shows the plots of each of these solutions.
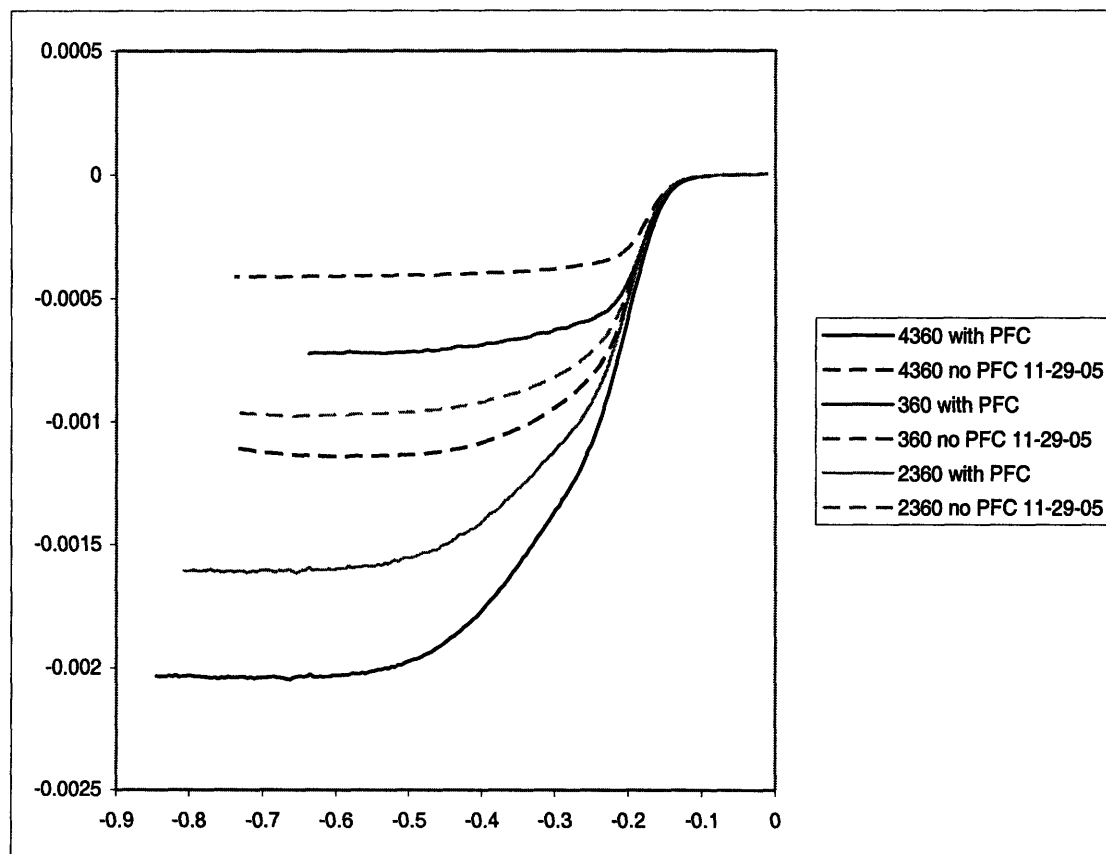
Figure 6. Current vs. Voltage plots of the six solutions run on the RDE

15

The benefit of using perfluorohexane relative to just the electrolyte mixture is summarized in Table 2. Additionally, the benefit of perfluorohexane determined by the RDE experiment is compared to the predicted increase in limiting current per the model developed earlier.

Table 2. The actual limiting current ratio for the perfluorohexane emulsion run using a RDE and the predicted current ratio using equation (22).

RPM	i_{PFC}/i_{OH} Predicted	i_{PFC}/i_{OH} Actual
360	3.75-4.75	1.71
2360	3.75-4.75	1.64
4360	3.75-4.75	1.83

4.4 Discussion of the results of the RDE experiment

Clearly there is consistency within the actual measured increase in current for the perfluorohexane emulsion, but the actual magnitude of the current increase is considerably lower than the model predicts. This section will address some of the potential non-idealities of the model, discuss the parameters used in the model, and touch upon some of the possible physical complications to the experiment.

First of all, the model simply assumes that the PFC's raise the effective concentration of the whole solution or spread across the disk electrode in a manner that creates an effective surface area subject to the bulk concentration. Both of these assumptions produce corresponding models; however, they are the ideal case.

The model for the limiting current in equation (9) depends on the known parameters for the diffusion layer. For the single electrolyte solution, this is straightforward; however, for the case when there is an emulsion, the situation becomes more complicated. For the predicted values in Table 2, the diffusion layer was assumed to be the same thickness in both cases. Perfluorohexane however has a lower kinematic viscosity than a solution of KOH [25], so the diffusion layer for the PFC emulsion solutions would be thinner than the case of the electrolyte alone. If this were incorporated into the model, the predicted value of the current ratio would be even higher than it is. This difference would be relatively small though since the kinematic viscosity of perfluorohexane is about .004 cSt whereas that of the electrolyte alone is on the order of .01 cSt. This would make the predicted value approximately 2% more than is shown in Table 2.

There are other factors that contribute to the actual current ratio being less than the predicted current ratio. The model in (12) and the inclusion of kinematic viscosity above assumes that the solution is uniform over the surface of the plate. In reality, the emulsion spheres are passing through the diffusion layer and over the electrode area. For an emulsion such as the one created for this experiment, the droplet size of the perfluorohexane varies throughout the solution. Even though the model assumes that the radius of the droplet does not affect the overall limiting current, if we look closer, this is probably not the case. If the thickness of the diffusion layer is on the order of the average droplet size, then droplets larger than the diffusion layer will face greater resistance to

reaching the electrode surface. Smaller droplets will be able to diffuse into the diffusion layer easier and reach the surface of the electrode with little resistance.

Additionally, when the model for the electrolyte was created, the assumption was a uniform concentration gradient across the diffusion layer. This works well for the single phase solution, but may not be as feasible for the emulsion. Assuming for the time being that the oxygen contribution from the perfluorohexane is high enough that we can neglect the contribution from the electrolyte and that a perfluorohexane sphere that reaches the electrode surface contributes all of its dissolved oxygen to the system, then the concentration gradient governing the mass transport realm of the model is no longer oxygen concentration through a solution. The diffusion of the perfluorohexane spheres onto the surface of the electrode determines how much oxygen can be reacted. Because this is a different mass transport problem, we may have reached the limitations of the model. Future research may be conducted to determine the relationship between droplet size and the diffusion coefficient of the PFC spheres. Once this is determined, an extension of the model can be made utilizing the diffusion coefficient of the PFC spheres and the Langmuir equation to predict the flux of oxygen onto the surface and subsequently the limiting current that would be present in the electrode.

Moreover, the contact of the PFC spheres with the electrolyte plate may not follow equation (15) derived in the model. In this case the boundary dimensions of the RDE setup would be needed to give a more accurate prediction of the limiting current. This error would be of a much smaller magnitude than those discussed above. If the other abnormalities can be accounted for, the approximation for the probability of contact may have to be expressed piecewise for setups of different dimensions. The approximation for the shape of the contact area may also be addressed since a PFC droplet that contacts the electrode surface will have a large shear force present on one side of the droplet and relatively little shear force on the opposite side. This could create PFC droplets that contact and "bounce" or roll off the electrode surface. This could also create PFC droplets that adhere to the electrode surface but become elongated as one side of the droplet is accelerated. Both of these considerations affect not only the model presented, but also a model as described in this section using the flux of PFC droplets across the electrode surface.

Another notable reason for the lower limiting current produced by the PFC emulsion than expected could be the type of reduction reaction that the oxygen is undergoing on the electrode surface. As described in section 3.0, there are two possible modes of oxygen reduction, one resulting in an $n = 4$ and the other resulting in $n = 2$. If the electrolyte solution consistently reacts to produce four electrons per oxygen molecule and the PFC emulsion produces two electrons per oxygen molecule, then the results would be similar to what was found in our experiment. The mode by which the two solutions would be dominated by different mechanisms has not been addressed. This could be analyzed by monitoring the RDE for the presence of hydrogen peroxide. Not only could this be a possible means for explaining the results obtained, but if true, it represents another mode of optimizing the system. Clearly it is beneficial to have oxygen fully reduced to

hydroxide, so any means of increasing the rate of the fully reducing reaction relative to the partially reducing reaction would create great increases in limiting current.

The surface interactions of the surfactant were not fully analyzed and may present a hindrance to mass transport that was not accounted for. This may only be an issue if the PFC droplet keeps the surfactant as a boundary between the PFC and the electrode. This is less of an issue if the droplet sheds the surfactant at the point of contact with the electrode. As a side not, the surfactant used does not present any direct advantages or disadvantages by itself except for displacing electrolyte carrying oxygen to the electrode. It can be seen in Figure 7 that for solutions of KOH with and without the surfactant, the limiting current is very close. This can be seen best in the 4360, 3360, and 360 rpm runs.
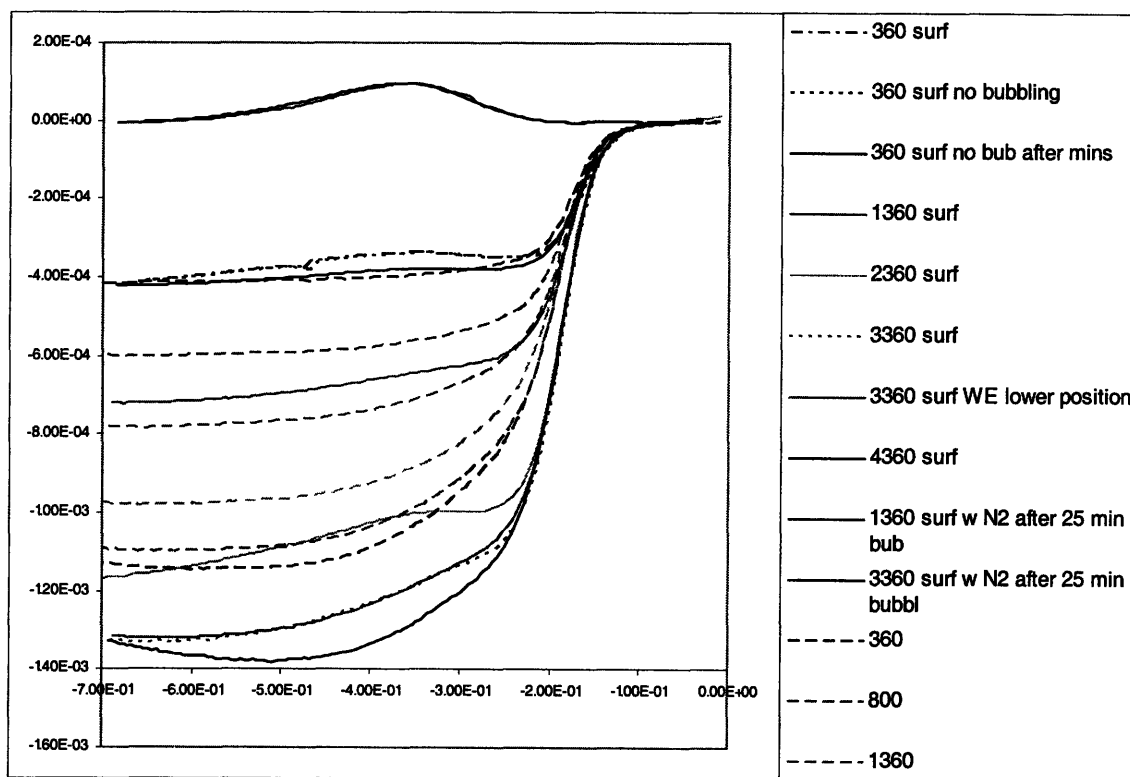
Figure 7. Current vs. Potential for the RDE experiment showing that the surfactant has little effect on the limiting current by itself

5.0 Screen Electrodes

The use of screen electrodes currently appears to be the most efficient means of harnessing the benefits of chemical pressurization due to fluidization. Current models for a single electrolyte solution produce results for screen electrodes that surpass two and three phase fluidized bed electrodes as well as packed electrodes. In the following section, a model for using a perfluorocarbon emulsion in conjunction with screen electrodes will be developed and then analyzed for defining parameters.

18

5.1 Linear Concentration Model

As the dissolved oxygen passes through the screen electrodes and is reduced, the oxygen concentration decreases causing the current harvested from the screens downstream of the flow to be smaller than the current collected at the first screen in the electrode. This concentration gradient also exists along the dimension of a single screen that is parallel to the direction of flow. The derivation of the differential equation for the modeling of this flow results in a concentration profile in the direction of fluid flow with the form [15]

$$C_{out} = C_{in} \cdot \exp\left(\frac{-k_m A L}{\dot{V}}\right) = C_{in} \cdot \exp\left(\frac{-k_m A_S}{\dot{V}}\right) \tag{23}$$

where the current consumed by the cell can be determined by the following equation

$$i = zF\left(C_{in} - C_{out}\right)\dot{V} \tag{24}$$

Combining equations (23) and (24), we can determine the limiting current produced by a screen electrode as a function of the concentration of oxygen entering the electrode, the surface area of the electrode (A_s), and the volumetric flow rate (V_dot)

$$i_{lim} = zF\dot{V}C_{sat}\left\{1 - \exp\left(\frac{-k_m A_S}{\dot{V}}\right)\right\} \tag{25}$$

For the electrode as a whole, we will assume that the concentration entering the cell is a saturated oxygen electrolyte.

5.2 Screen Electrode Mass Transfer Model

To model the mass transfer over the screen, the experimental value for the Sherwood number determined by Holeschovsky et al [19] is used

$$Sh = .82(Sc)^{.33}(\mathrm{Re})^{.359} \tag{26}$$

The Schmidt and Reynolds numbers take the form below

$$Sc = \frac{\mu}{\rho_f D_{O_2}} \tag{27} \qquad\qquad \mathrm{Re} = \frac{\rho_f U_{sf} d_{wire}}{\mu} \tag{28}$$

By substituting the dimensionless numbers into equation (26), the mass transfer coefficient can be solved for.

$$k_{Screen} = \frac{.82 * D_{O_2}}{d_{wire}} * \left(\frac{\mu}{\rho_f D_{O_2}}\right)^{0.33} * \left(\frac{\rho_f U_{sf} d_{wire}}{\mu}\right)^{0.359} \tag{29}$$

The mass transfer coefficient can be combined with equation (25) to produce an overall equation for the limiting current in a screen electrode where A_H and b_H are constants determined from [19] discussed earlier.

$$i_{lim} = zF\dot{V}C_{sat}\left\{1-\exp\left[\frac{-D_{O_2}A_SA_H}{d_{wire}\dot{V}}\left(\frac{\mu_f}{\rho_fD_{O_2}}\right)^{0.33}\left(\frac{\rho_fU_{sf}d_{wire}}{\mu}\right)^{b_H}\right]\right\} \quad (30)$$

The independent variables in equation (30) can be reduced to the volumetric flow rate and the diameter of the screen mesh. The limiting potential is clearly increasing in both volumetric flow rate and wire diameter. This can be seen by figure 8 which shows a steady increase in current by increasing both parameters.

Limiting current as a Function of the Screen Mesh Diameter and the Volumetric Flow Rate
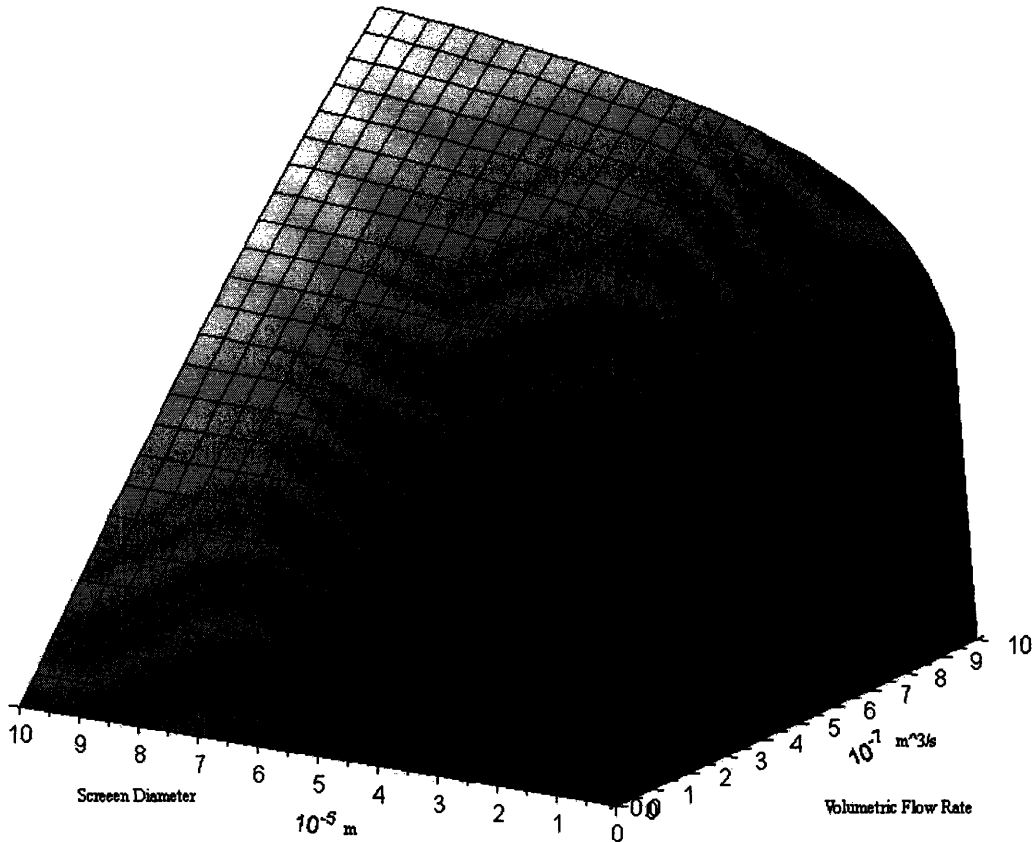
Figure 8. 3D Plot of the limiting current from equation (30) as a function of the volumetric flow rate and the screen diameter.

The mesh screen used as a primer for this model is a platinum catalyst mesh screen manufactured by UNIQUE Wire Weaving Company. Ruflin summarizes the properties of this screen and the table is reproduced below. A discussion of how the screen dimensions relate is also include by Ruflin [15].

20

Table 3. Characteristics of UNIQUE Wire Weaving Company's plantinum screen used in this portion of the screen electrode model.

Mesh (wires/inch)	Wire Diameter (mm)	Width of Opening (mm)	Surface Area/ Total Area	% Open Area, $\overline{f}$
150 x 150	0.0432	0.127	1.6	55.5

The power output from a screen producing a limiting current is determined by the potential that is sustainable at that current. To keep consistency in this portion of the model, the value for the potential of .8 V used by Ruflin will be used [15]. This value seems to be an upper limit to the potential of a fluidized bed electrode and serves as a good approximation of the potential that would be found in the screen electrode system.

By increasing the volumetric flow rate, the amount of oxygen that passes over the electrode in any given time period increases, increasing current, and also decreases the concentration gradient in the direction of the flow. A higher concentration of oxygen is maintained throughout the entire cell. An increase in the wire mesh diameter would cause a higher Reynolds number resulting in better mass transport. In addition, the surface area of the electrode would be increased for each screen present. However, as the diameter of the wire increases, the velocity of the electrolyte flowing past the screen must increase. This in turn increases the Reynolds number enough that eventually this model breaks down. An optimization of the limiting current with respect to the wire diameter must provide an optimal wire diameter because in the limiting case that the wire diameter approaches the length of the opening, no more electrolyte will pass through the cell and the limiting current would go to zero.

More important than the limiting current is the actual power output of the cell. The limit of the power generated by the cell is just the multiplication of the current and potential.

$$P_{gen} = i_{\lim} * E \tag{31}$$

However, what is of concern is the net power output of the cell which takes into account the energy required to pump the electrolyte through the electrode.

5.3 Net Power Output of Screen Electrodes

The model created by Ruflin to analyze the net power loss utilizes the increase in velocity across the screen as a result of the restricted flow created by the screen. The velocity within the electrode can be described by the relationship [15]

$$U_{ws} = \frac{U_{sf}}{f} \tag{32}$$

The fraction of the cross-sectional area of the screen that is open to flow is given by (f). The Reynolds number for the flow in the screen electrode is determined by

$$Re_{ws} = \frac{\rho_f U_{ws} d_{wire}}{\mu} \tag{33}$$

The pressure drop over any one screen is therefore given by the relationship [15]

$$\Delta p_{screen} = \frac{\rho U_{sf}^{2}}{2} \left(\frac{22}{Re_{ws}} + \zeta_{wire} \right) \tag{34}$$

where (ζ_{wire}) is a dimensionless pressure drop that is characteristic of the screen. The length of the entire packed screen bed can be given by

$$L_{Electrode} = N_{Screens} * w_{Screen} = 2 * N_{Screens} * d_{wire} \tag{35}$$

Ideally, the power dissipated by the pump is going to be equal to the volumetric flow rate times the pressure drop over the electrode.

$$P_{Pump} = \dot{V} * \Delta p_{total} = \dot{V} * \Delta p_{screen} * N_{screens} \tag{36}$$

Combining equations (31) and (36) we arrive at a net power output [15]

$$P_{Net} = P_{Gen} - P_{Pump} \tag{37}$$

In order to optimize, the effective electrode surface area is defined as the active electrode area of one screen times the number of screens in the packed bed

$$A_s = 2 * \pi * d_{wire} * L_{mesh} * N_{Screens} \tag{38}$$

In addition, the total bed length can be defined as

$$L_{Bed} = w_{Screen} * N_{Screens} = 2 * d_{wire} * N_{Screens} \tag{39}$$

By substituting equations combining the equations above, the net power output, P_{net} can be optimized with respect to the length of the packed screen bed and the volumetric flow rate. A 3D plot of the maximization is shown below in Figure 9. The optimal power output is obtained at a volumetric flow rate of 2.4e-8 cubic meters per second through a cross sectional area of 4.55e-8 square meters. This results in a superficial velocity of .527 meters per second. This is significantly higher than velocity of flows used in fluidized bed experiments. Additionally, the length of the bed is larger than predicted by Ruflin [15] using only an electrolyte oxygen carrier. The optimal length of the packed screen electrode is approximately 7 cm.
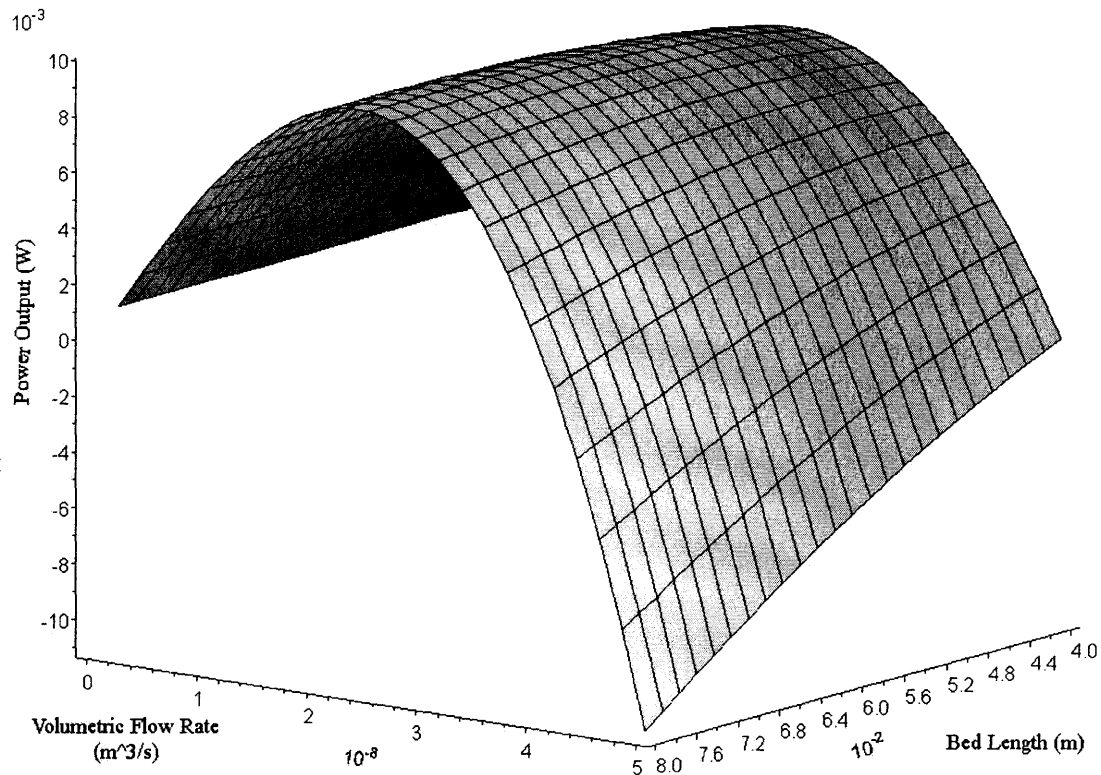
Figure 9. Optimization of the net power output of a packed screen electrode with respect to volumetric flow rate and bed length. For $C_{sat} = 2$, the maximum power output is obtained with a bed length of 7.2 cm and a volumetric flow rate of 2.4e-8 cubic meters per second.

5.4 Application of Screen Electrodes to PFC emulsions

The power consumed by the pump is completely a function of the flow parameters and is not affected by the amount of oxygen dissolved in the system. The power put out by the electrode, on the other hand, is linearly proportional to the concentration of oxygen in the electrolyte. As we have shown above in the RDE experiment, there is a clear benefit for fuel cell applications of adding PFC's to the electrolyte to chemically pressurize the system raising the oxygen concentration and the power output of the cell. When optimizing the net power output, it can be seen that as the concentration of oxygen increases, the optimal length of the bed increases and the optimal volumetric flow rate increases.

What follows from the model is that the use of PFC's to chemically pressurize the electrolyte will allow for the use of longer electrodes and higher flow rates. The longer electrodes will lend themselves to a better overall power output density by being able to make an electrode with more surface area relative to the bulk volume of the whole cell. That is, a greater portion of the cell volume will be occupied by current producing electrode. In addition, the higher volumetric flow rate will increase the power output

density. The electrolyte that cycles through the cell will be able to come in contact with the electrode more often with a higher volumetric flow rate, delivering more oxygen to the electrode and thus more power output for a given cell volume. From the analysis performed, the increase in power output of the screen electrode cell should be on the same order of magnitude as the increase in oxygen saturation due to the addition of PFC's if the parameters of the cell are optimized for the expected oxygen concentration. The implications of this are that the fluidized approach to fuel cells has the potential to create a much higher power output density than current PGD fuel cells. Figure 10 shows the power output optimization for $C_{sat} = 200$ for illustration purposes. The optimal volumetric flow rate for this hypothetical system is 1.1e-7 [m^3/s] and the optimal bed length is 18 cm. The flow is 20 times greater in this case than in Figure 9 and the bed is over twice as long. The power output is also 2 orders of magnitude greater in this case.
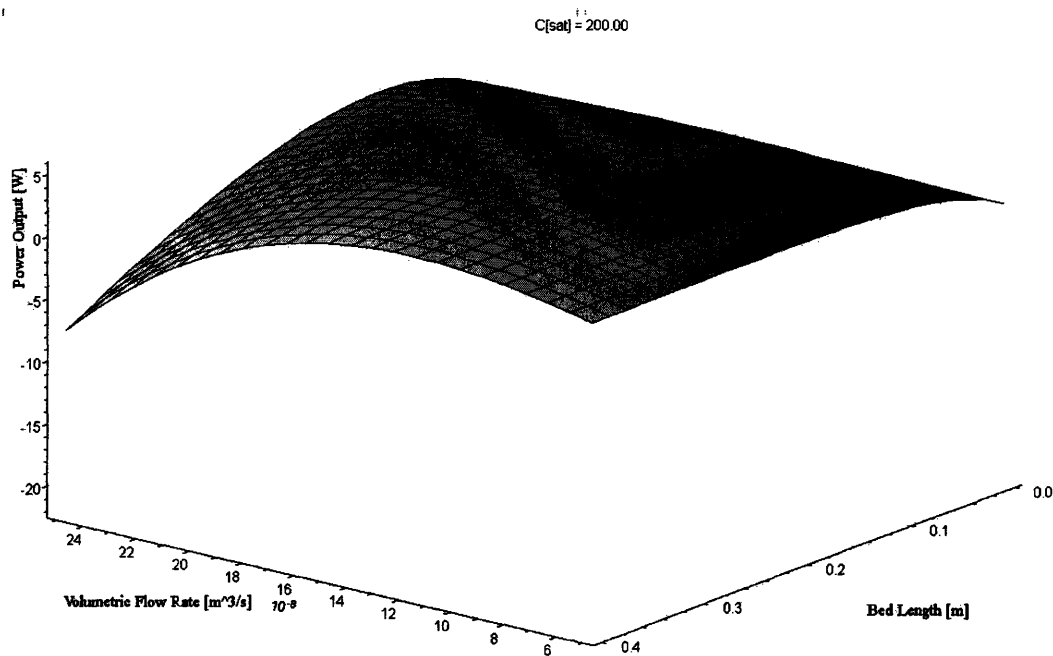
Figure 10. Hypothetical case of 200 times the oxygen concentration of .5M saturated KOH electrolyte. This illustrates the effect of higher concentration on bed length and volumetric flow rate.

5.5 Probabilistic Model

As discussed in the case of the RDE, the PFC emulsion may not be best modeled by using an effective oxygen concentration, but rather a probabilistic model of whether or not an emulsion sphere is able to come in contact with the electrode. Future research could create a model which is able to apply the ideology developed in section 3.1 to a 2D and 3D packed screen electrode model.

6.0 Design of Screen Electrode for Future Research

In order to first test the effect of PFC emulsions on a characteristic screen electrode bed, an oxygen half cell setup was created which included a reactant well for stacking screen electrodes, a standing well for the reference electrode, a counterflow oxygen saturator, a peristaltic pump so that there is no contact between the pump parts and the electrolyte, and a dampener to create a steady flow of electrolyte through the screen electrode. Figures 11 and 12 show the electrode cell and reference electrode well that will be used to collect data for comparison with the model above and its extensions. Figure 13 shows the peristaltic pump, Figure 14 shows the mercury oxide reference electrode, and Figure 15 shows platinum screen.

Figure 11. Screen electrode cell. Electrolyte flows through threaded port on left which is filled with packed screens. Electrolyte proceeds to reference electrode well, then exits through port on right and into oxygen saturator.
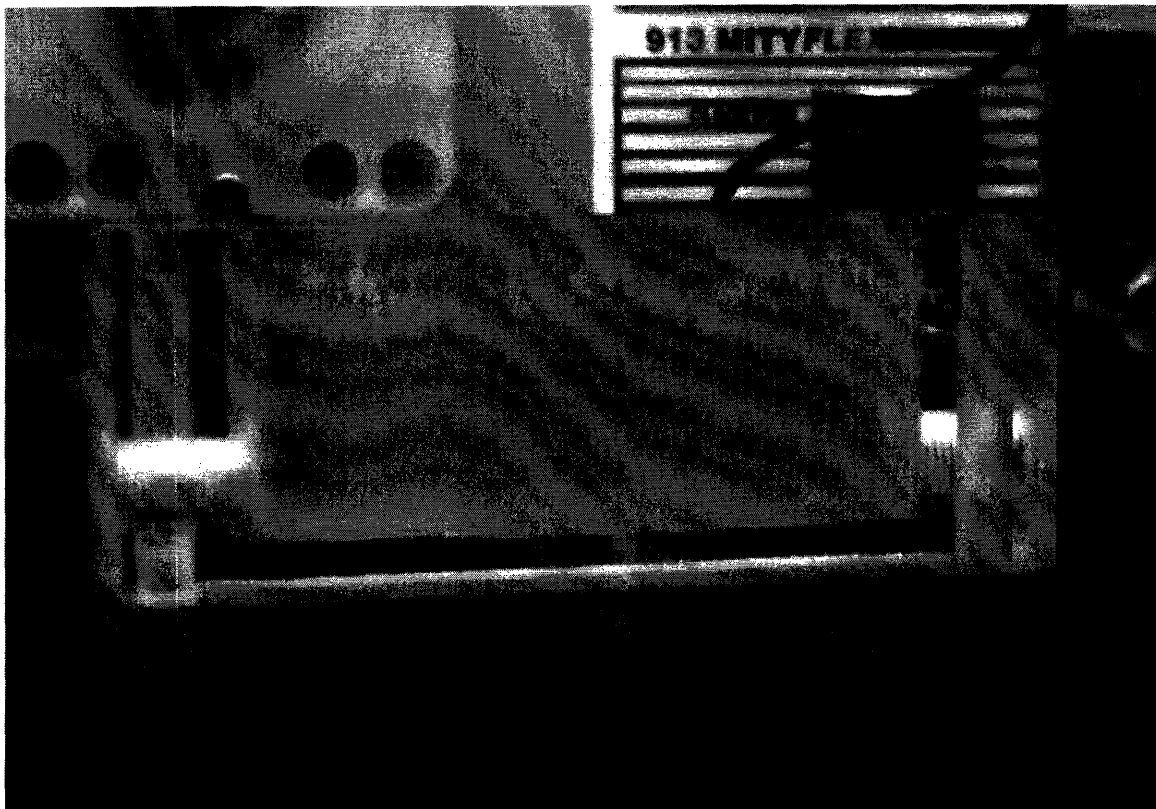
Figure 12. Screen electrode cell and reference electrode well.
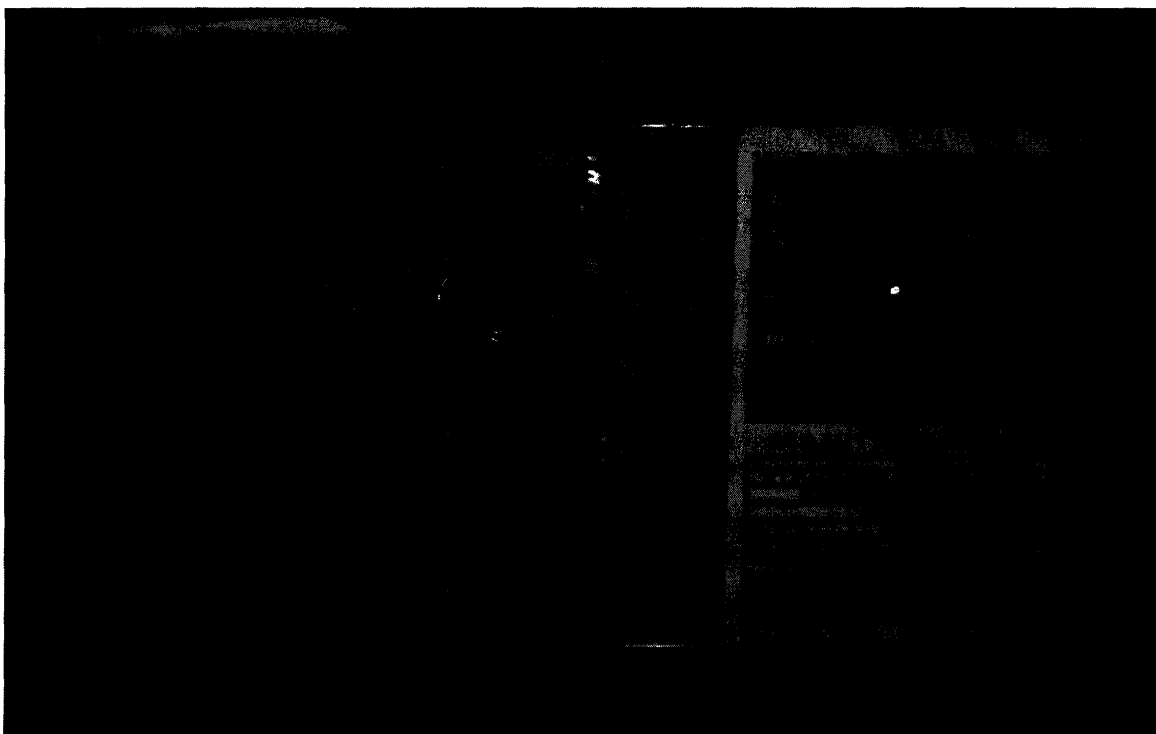
Figure 13. MITYFLEX Peristaltic pump 913 used to test screen cell electrode.

Figure 14. Koslow Scientific mercury oxide reference electrode used to test screen electrode.

Figure 15. Platinum screen electrode for use in testing screen electrode

The peristaltic pump used is a MITYFLEX model number 913. The mesh screens were fabricated by UNIQUE Wire Weaving Company and are detailed in Table 3. Additional tests may be conducted using Aldrich platinum gauze, 100 mesh, 99.9%. The oxygen saturator (not depicted) is a spiral counterflow design in which pure oxygen gas is passed over the electrolyte that has just exited the electrode. The reference electrode was a mercury oxide reference electrode (P/N 5088) made by Koslow Scientific. The cell structure and electrode well were created out of polycarbonate purchased from McMaster and were milled using waterjet and CNC technology.

This experimental setup can be used to test the effects of stacking screens in the electrode similar to what was modeled earlier in this thesis. The orientation of the stacked screens can also be analyzed and modeled accordingly. Furthermore, the characteristics of the PFC emulsion can be varied. Average drop diameter and dispersion can be used as independent variables to test their effect on the overall cell power output.

Finally, on a more macro scale, the setup can be rebuilt to further optimize power output given the additional data. This half cell can then be included in a full fuel cell to get a realistic representation of its feasibility in industry relative to PGD fuel cells.

6.1 Additional Future Research and Model Extensions

Future research, in addition to what is described above, could be performed to better understand the interaction of the PFC emulsion droplets with the electrode. A more accurate representation of the effective concentration and surface area would allow for better predictions of fuel cell output and efficiency. One such possibility would be to conduct research to determine the relationship between droplet size and the diffusion coefficient through an electrolyte medium.

Furthermore, other perfluorocarbons could be analyzed to account for their feasibility in fuel cell applications. Also, future work could be performed to understand the effects of PFC's, which have a high solubility for carbon dioxide, on the type of catalyst used in the electrode. Catalyst poisoning may progress much faster using PFC's if the effects are not mitigated. Finally, an optimization that includes the cost of the cell including the catalyst with respect to cell bed length would also be an important area of research. Optimizing cost effectiveness is as important as optimizing power output because no matter how efficient, if the technology is not economical, it will not be used in practice.

References

1. "Petroleum," Online Data, <u>Energy Information Administration</u>, 2007 <http://www.eia.doe.gov/oil_gas/petroleum/info_glance/petroleum.html>.
2. "Title 49, United States Code..." Online Data, <u>Department of Transportation</u>, 2007 < http://www.nhtsa.dot.gov/nhtsa/Cfc_title49/ACTchap321-331.html>.
3. I. Bar-On, R. Kirchain, R. Roth, "Technical cost analysis for PEM fuel cells," <u>J. Power Sources</u>, vol. 109, 71-75, 2002.
4. J. Scholta, N. Berg, P. Wilde, L. Jorissen, and J. Garche, "Development and performance of a 10 KW PEMFC stack," <u>J Power Sources</u>, vol. 127, pp. 206-212, 2004.
5. M. Cropper, S. Geiger, D. Jollie, "Fuel cells: a survey of current developments," <u>J Power Sources</u>, vol. 131, pp. 57-61, 2004.
6. E. Middelman, W. Kout, B. Vogelaar, J. Lenssen, E. de Waal, "Bipolar plates for PEM fuel cells," <u>J. Power Sources</u>, vol. 118, pp. 44-46, 2003.
7. A. Heinzel, F. Mahlendorf, O. Niemzig, C. Kreuz, "Injection moulded low cost bipolar plates for PEM fuel cells," <u>J. Power Sources</u>, vol. 131, pp. 35-40, 2004.
8. M. Eikerling, A. Ioselevich, A. Kornyshev, "How good are the Electrodes we use in PEFC?," <u>Fuel Cells</u>, vol. 4, No. 3, 2004.
9. S. Kamarudin et al., "Design of a Tubular Ceramic Membrane for Gas Separation in a PEMFC System," <u>Fuel Cells</u>, vol. 3, No. 3, 2003.
10. K. Matsuoka, Y. Iriyama, T. Abe, M. Matsuoka, Z. Ogumi, "Alkaline direct alcohol fuel cells using an anion exchange membrane," <u>J. Power Sources</u>, vol. 150, pp. 27-31, 2005.
11. M. Schonert et al., "Manufacture of Robust Catalyst Layers for the DMFC," <u>Fuel Cells</u>, vol. 4, No. 3, 2004.
12. G.F. McLean., T. Niet, S. Prince-Richard, N. Djilali, "An assessment of alkaline fuel cell technology," <u>Int. J Hydrogen Energy</u>, vol. 27, pp. 507-526, 2002.
13. E. Gulzow, M. Schulze, "Long-term operation of AFC electrodes with CO_2 containing gases," <u>J. Power Sources</u>, vol. 127, pp. 243-251, 2004.
14. J. Jo, S. Yi, "A computational simulation of an alkaline fuel cell," <u>J. Power Sources</u>, vol. 84, pp. 87-106, 1999.
15. Ruflin, J. (2006). *The Performance of Fluidized Beds, Packed Beds, and Screens as Fuel Cell Electrodes*. Master's Thesis, Massachusetts Institute of Technology, Boston, MA.
16. Y. Matsuno, K. Suzawa, A. Tsutsumi, K. Yoshida, "Characteristics of three-phase fluidized-bed electrodes for an alkaline fuel cell cathode," <u>Int. J. Hydrogen Energy</u>, vol. 21, pp. 195-199, 1996.
17. M. Eikerling, A.S. Ioselevich, A.A. Kornyshev, "How good are the electrodes we use in PEFC?" <u>Fuel Cells</u>, vol. 4, pp. 131-140, 2004.
18. Y. Matsuno, A. Tsutsumi, K. Yoshida, "Improvement in electrode performance of three-phase fluidized-bed electrodes for an alkaline fuel cell cathode," <u>Int. J. Hydrogen Energy</u>, vol. 22, pp. 615-620, 1997.
19. U. Holeschovsky, J. Tester, W. Deen, "Flooded flow fuel cells: a different approach to fuel cell design," <u>J. Power Sources</u>, vol. 63, pp. 63-69, 1996.

20. D. Spahn, "Blood substitutes Artificial oxygen carriers: perfluorocarbon emulsions," <u>Critical Care</u>, vol. 3, no. 5, pp. R93-R97, 1999.
21. M. Freire et al., "Enzymatic method for determining oxygen solubility in perfluorocarbon emulsions," <u>Fluid Phase Equilibria</u>, vol. 231, pp. 109-113, 2005.
22. J. Prentice, H. Craig, "Rotating Disk Electrode Oxygen Sensor and Corrosion Rate Probe," <u>J. Ocean Engineering</u>, vol. OE-4, no. 4, pp. 137-141, 1979.
23. J. Reiss, "Oxygen Carriers ("Blood Substitutes") – Raison d'Etre, Chemsitry, and Some Physiology," <u>Chem. Rev.</u>, vol. 101, pp. 2797-2919, 2001.
24. K. Lowe, "Perfluorochemical respiratory gas carriers: benefits to cell culture systems," <u>J. Fluorine Chemistry</u>, vol. 118, pp. 19-26, 2002.
25. M. Freire et al., "Aging mechanismsof perfluorocarbon emulsions using image analysis," <u>J. Colloid and Interface Science</u>, vol. 286, pp. 224-232, 2005.